Moment of Inertia Identification Using the Time Average of the Product of Torque Reference Input and Motor Position

Fukashi Andoh, *Member, IEEE*

***Abstract*—This paper is concerned with moment of inertia identification of mechatronic servo systems with limited strokes. The moment of inertia identification algorithm proposed in this paper utilizes periodic position reference input, and identifies moment of inertia of mechatronic servo systems based on the time average of the product of torque reference input and motor position. Simulations and experiments on two mechatronic servo systems suggest the effectiveness of the proposed algorithm on mechatronic servo systems with limited strokes.**

***Index Terms*—Antiresonance, backlash, control gain tuning, inverters, moment of inertia, motion control, resonance, single-degree-of-freedom (SDOF) systems, servomotors, system identification, two-degree-of-freedom (2DOF) systems.**

I. Introduction

MANUFACTURING premises have been increasingly more automated to protect human workers from hazardous environment, reduce manufacturing time and cost, and manufacture extraordinarily precise and small electronic devices and machine elements that cannot be manufactured manually. Many of the automated manufacturing devices used today are mechatronic servo systems, controlled electromechanical systems designed based on mechanics, electronics and computing. Chip mounters, LCD manufacturing devices, machine tools and welding robots fall under this umbrella. Such mechatronic servo systems are required to have fast and precise motions, and the required speed and precision continue to grow in the pursuit of even higher productivity, smaller electronic devices, higher quality LCD panels and finer machine elements. To orchestrate the motions of mechatronic servo systems in such a manner, a variety of motion control strategies have been investigated [1]–[7].

In many of the motion control applications system structures of the mechatronic systems to be controlled are known, whereas their system parameters are unknown. For example robot arms in manufacturing premises are often required to move in a desired manner when moment of inertia of workpieces is not given. As the requirements of the speed and precision of the motions of manufacturing devices become more and more stringent, prior knowledge about the system parameters is of great advantage in designing motion control. For this reason numbers of system identification algorithms have been proposed and studied [8]–[28].

Among the system parameters, moment of inertia is an essential parameter in torque feedforward controllers and often a normalizing factor of feedback control gains in the servo drivers for industrial robots. With the identification of moment of inertia, control design is simplified, and the same normalized control gains can be used to provide almost the same dynamic responses satisfying high speed high precision requirements in various mechatronic servo systems under different loading conditions.

Existing works related to moment of inertia identification utilize observers [29]–[36], Kalman filter [37] and adaptation algorithms [38]–[40]. Observer based algorithms calculate moment of inertia based on some variables estimated by an observer such as estimated motor speed and estimated torque disturbance. Kalman filter based algorithm treats moment of inertia as one of the state variables and obtains moment of inertia as a direct output from Kalman filter. Adaptation based algorithms vary moment of inertia in a mathematical model until estimated motor speed converges to the actual motor speed.

In this paper, an off-line moment of inertia identification algorithm of mechatronic servo systems with limited strokes using the time average of the product of torque reference input and motor position is introduced. The first part of this paper shows a derivation of the proposed identification algorithm. The remaining part of this paper demonstrates the effectiveness of the proposed identification algorithm on nonrestrained single-degree-of-freedom (SDOF) systems and nonrestrained two-degree-of-freedom (2DOF) systems based on the simulations and experiments on an electric motor and a linear slider.

II. Moment of Inertia Identification Algorithm

This section introduces a moment of inertia identification algorithm. The proposed identification algorithm identifies moment of inertia of a motor with mechanical load using torque reference input and motor position as in Fig. 1. Torque reference input is sent to the driver that generates motor current to drive the motor with load. The encoder attached to the motor measures motor position, and moment of inertia is identified using torque reference input and motor position. Although the derivation of the proposed identification algorithm in what follows is based on rotational motors, the proposed algorithm is also applicable to linear motors using an analogy between rotational mechanical systems and translational mechanical systems [41].

Assuming the case when elastic body dynamics of the motor with load in Fig. 1 is not dominant, the motor with load can

Manuscript received October 25, 2006; revised December 7, 2006. Recommended for publication by Associate Editor J. Ojo.

The author is with the Yaskawa Electric Corporation, Fukuoka 803-8530, Japan (e-mail: fandoh@yaskawa.co.jp).

Digital Object Identifier 10.1109/TPEL.2007.909309

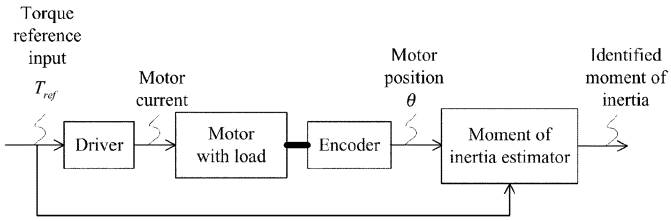

Fig. 1. Block diagram of moment of inertia estimator.

be approximated by a nonrestrained single-degree-of-freedom (SDOF) system, and its equation of motion becomes

$$J\ddot{\theta} + D\dot{\theta} = T_{\text{ref}} - w \tag{1}$$

where J is moment of inertia of the motor with load, D is viscous friction, T_{ref} is torque reference input, θ is motor position and w is constant torque disturbance. Constant torque disturbance appears when the orientation of the mechanical load is such that gravitational acceleration rotates the rotor of the motor.

Letting torque reference input a sinusoidal signal of frequency ω, motor position becomes a sinusoidal signal of the same frequency ω at steady state and can be expressed as

$$\theta = A\cos\omega t \tag{2}$$

where A is amplitude of motor position. In (2) phase of motor position is ignored because only relative phase between torque reference input and motor position has an effect on the identification result. Using (1) and (2) torque reference input is expressed as

$$T_{\text{ref}} = -\omega^2 \text{AJ}\cos\omega t - \omega \text{AD}\sin\omega t + w. \tag{3}$$

Using (2) and (3) the product of torque reference input and motor position is calculated as

$$\begin{aligned} T_{\text{ref}}\theta &= -\omega^2 A^2 J\cos^2\omega t - \omega A^2 D\cos\omega t\sin\omega t \\ &\quad + wA\cos\omega t \\ &= -\omega^2 A^2 J\left(\frac{1}{2}\cos 2\omega t + \frac{1}{2}\right) \\ &\quad - \omega A^2 D\frac{1}{2}\sin 2\omega t + wA\cos\omega t. \end{aligned} \tag{4}$$

Right hand side of (4) consists of two sinusoidal terms of period π/ω, one sinusoidal term of period $2\pi/\omega$ and one constant term. Taking the time average of (4) over one period $T_p = 2\pi/\omega$ and solving it for moment of inertia J yield

$$J = -\frac{2\overline{T_{\text{ref}}\theta}}{\omega^2 A^2} \tag{5}$$

where bar denotes the time average over one period. The derivation of (5) utilized that the time average of three sinusoidal terms in (4) vanishes. The proposed identification algorithm calculates moment of inertia of the motor with load using (5). Although the derivation of identification equation (5) above assumed sinusoidal torque reference input, the proposed algorithm can be applied for general periodic torque reference inputs of period $T_p = 2\pi/\omega$. In such cases, fast Fourier transform (FFT) is used to extract the fundamental frequency component, a frequency component of frequency ω, from periodic torque reference input and motor position, and the fundamental frequency component of torque reference input and that of motor position are used in (5) to identify moment of inertia.

The advantages of the proposed algorithm are summarized as follows.

1) The identification equation (5) uses torque reference input and motor position, and does not contain control parameters explicitly. Therefore, the proposed algorithm can be used with any linear control law.
2) When the fundamental frequency component of torque reference input and that of motor position are used in (5), other frequency components do not affect the identification result, and the proposed algorithm can be used with any periodic reference input containing the frequency component necessary to the identification.
3) For the same reason as 2), by using the fundamental frequency component in (5), the effect of noise, superharmonics and subharmonics due to nonlinear dynamics such as backlash and Coulomb friction on the identification result is reduced.
4) For the same reason as 2), by using the fundamental frequency component in (5), frequency components of transient response are eliminated and identification can be started without waiting the transient response to die out. Hence, with the proposed algorithm, the time for acquiring torque reference input and motor position for identification calculation is short.
5) When the amplitude of motor position is infinitesimal and the waveform of motor position is not smooth because of encoder resolution, the peak-to-peak amplitude of motor position is reduced. In such a case, motor position is smoothed by taking FFT and its amplitude is recovered to some extent. Hence, the proposed algorithm is suitable for moment of inertia identification with infinitesimal motions.
6) When sampling time is long, number of sampled points per period is reduced. In such a case, the phase of torque reference input and the phase of motor position after applying FFT are shifted by the same amount. Since relative phase between torque reference input and motor position remains unchanged, relatively long sampling time does not affect the identification result.
7) When sampling time is long, the amplitude of torque reference input and that of motor position are reduced for the same reason as 6. In such a case, the rate of the amplitude reduction of torque reference input and that of motor position are the same, and their effect on the identification result cancels in (5). Therefore, the proposed algorithm can be used with controllers and drivers of relatively long sampling time.

III. Simulations and Experiments

In the previous section a moment of inertia identification algorithm is introduced. This section discusses the applicability of the proposed identification algorithm to nonrestrained single-

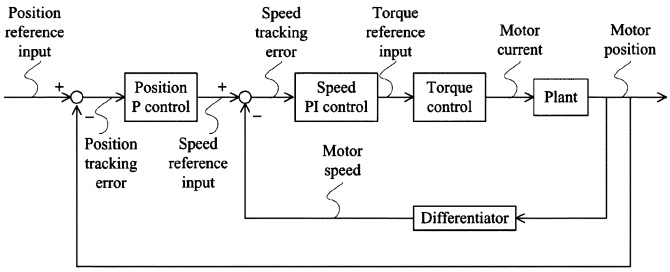

Fig. 2. Position P speed PI controlled motor with load.

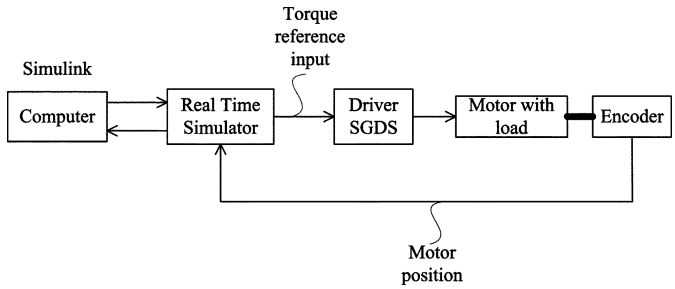

Fig. 3. Experimental setup with Real Time Simulator.

degree-of-freedom (SDOF) systems, and nonrestrained two-degree-of-freedom (2DOF) systems with simulations and experiments on an electric motor and a linear slider.

A. Simulation Conditions

Simulations utilize a block diagram in Fig. 2 constructed on Simulink. In Fig. 2 position proportional speed proportional integral (position P speed PI) control is used to generate torque reference input as widely used in servo products. Plant consists of the motor with load and the encoder. The motor with load is written in continuous time, and the rest of the closed loop system in Fig. 2 is written in discrete time with sampling time T. The encoder is written as a quantization block representing its resolution. In simulations two cases are considered: (a) elastic body dynamics of the motor with load is negligible, and (b) elastic body dynamics of the motor with load is not negligible. For case (a) the motor with load is represented by an SDOF system, and for case (b) the motor with load is represented by a 2DOF system. For cases (a) and (b) transfer function $G_p(s)$ of the motor with load without motor viscous friction and Coulomb friction is expressed as (6) and (7), respectively,

$$G_p(s) = \frac{1}{Js^2} \tag{6}$$

$$G_p(s) = \frac{1}{Js^2}\frac{{\omega_r}^2}{{\omega_a}^2}\frac{s^2 + 2\zeta_a\omega_a s + \omega_a^2}{s^2 + 2\zeta_r\omega_r s + \omega_r^2} \tag{7}$$

where J is moment of inertia of the motor with load, ω_a is antiresonance frequency, ζ_a is damping ratio of antiresonance, ω_r is resonance frequency, and ζ_r is damping ratio of resonance. In the subsequent simulations the motor with load is represented by (6) and (7) with motor viscous friction $D\dot{\theta}$ and Coulomb friction $T_c\mathrm{sgn}(\dot{\theta})$. Torque reference input and motor position generated in Simulink are stored in a data file, and the calculation of moment of inertia is performed on Matlab using the data file.

B. Experimental Setups

Experiments utilize an experimental setup with Real Time Simulator in Fig. 3. DSP Technology Real Time Simulator is a software hardware package that interfaces Simulink and real life systems. Position P speed PI control as in Fig. 2 is constructed on Simulink, and torque reference input generated in Simulink is sent to the driver via Real Time Simulator. The driver drives the motor with load, and motor position measured by the encoder is fed back to the computer via Real Time Simulator. Torque reference input and motor position fed back from the encoder are stored in a data file, and the calculation of moment of inertia is performed on Matlab using the data file.

TABLE I
SPECIFICATIONS OF SYSTEM 1 (MOTOR ONLY)

Motor moment of inertia J_m	$0.116\times10^{-4}\ kg\cdot m^2$
True value of moment of inertia J^*	$0.116\times10^{-4}\ kg\cdot m^2$
Ratio of total moment of inertia to motor moment of inertia r_J	1
Viscous friction D	$0.75\times10^{-4}\ N\cdot m\cdot s/rad$
Coulomb friction T_c	$6.6\times10^{-3}\ N\cdot m$
Rated torque T_{rat}	$0.637\ N\cdot m$
Encoder resolution b	$17\ bit$
Power p	$200\ W$
Constant torque disturbance w	$0\ N\cdot m$

C. Systems Used in Simulations and Experiments

In simulations and experiments the following two systems are employed as examples of the motor with load

System1 : motor only
motor : YASKAWA SGMAS − 02ACA21
driver : YASKAWA SGDS − 02A01A
System2 : motor + slider
system 1 plus linear slider
(THK KR4620A + 540L slider,
Sakai ManufacturingUA − 35C coupling).

System 1 is an example of an SDOF system and system 2 is an example of a 2DOF system.

D. Specifications

The specifications of systems 1 and 2 are given in Tables I and II. True value of moment of inertia is calculated based on the material properties and the geometry of the motor, the linear slider and the coupling. Rated torque, encoder resolution and power are based on the motor and the driver used in systems 1 and 2. Resonance frequency and antiresonance frequency are measured using YASKAWA SigmaWin. Damping ratios are calculated from the quality factor of resonance and antiresonance peaks in the frequency response taken by YASKAWA SigmaWin. Viscous friction, Coulomb friction and constant torque disturbance are obtained experimentally using least square method as follows.

The motor with load is controlled by speed P control with speed P control gain given in Table III. Step speed reference

TABLE II
SPECIFICATIONS OF SYSTEM 2 (MOTOR + SLIDER)

Motor moment of inertia J_m	$0.116\times10^{-4}\ kg\cdot m^2$
True value of moment of inertia J^*	$0.556\times10^{-4}\ kg\cdot m^2$
Ratio of total moment of inertia to motor moment of inertia r_J	4.79
Viscous friction D	$0.96\times10^{-3}\ N\cdot m\cdot s/rad$
Coulomb friction T_c	$2.1\times10^{-2}\ N\cdot m$
Resonance frequency ω_r	$628.9(2\pi)\ rad/s$
Damping ratio of resonance ζ_r	0.05
Antiresonance frequency ω_a	$402.3(2\pi)\ rad/s$
Damping ratio of antiresonance ζ_a	0.05
Rated torque T_{rat}	$0.637\ N\cdot m$
Encoder resolution b	$17\ bit$
Power p	$200\ W$
Constant torque disturbance w	$0\ N\cdot m$

TABLE III
CONTROL PARAMETERS

Position P control gain K_p	$40\ s^{-1}$
Normalized speed P control gain K_v	$40(2\pi)\ s^{-1}$
Speed P control gain $K_{vj}=K_vJ_m$	$0.0029\ kg\cdot m^2/s$
Speed control integration time constant $T_i=4/K_v$	$0.016\ s$
Sampling time T	$125\times10^{-6}\ s$

input with constant speed v is inputted to the speed P controlled motor with load. At steady state the motor speed converges to $\dot{\theta}=v$ and equation of motion in (1) with Coulomb friction term is rewritten as

$$Dv+T_c\mathrm{sgn}(v)=T_{\mathrm{ref}}-w. \tag{8}$$

Letting $T_{\mathrm{ref1}+},T_{\mathrm{ref2}+},\ldots,T_{\mathrm{refn}+}$ be torque reference inputs for positive motor speeds $v_{1+},v_{2+},\ldots,v_{n+}$ respectively, (8) is rewritten as

$$\begin{aligned} T_{\mathrm{ref1}+}&=Dv_{1+}+T_c+w\\ T_{\mathrm{ref2}+}&=Dv_{2+}+T_c+w\\ &\vdots\\ T_{\mathrm{refn}+}&=Dv_{n+}+T_c+w. \end{aligned} \tag{9}$$

Rewriting (9) in a matrix form yields

$$\begin{aligned} \boldsymbol{T}_{\mathrm{data}+}&=\boldsymbol{A}_+\boldsymbol{x}_+\\ \boldsymbol{T}_{\mathrm{data}+}&=\begin{bmatrix}T_{\mathrm{ref1}+}\\ \vdots\\ T_{\mathrm{refn}+}\end{bmatrix},\boldsymbol{A}_+=\begin{bmatrix}v_1+ & 1\\ \vdots & \vdots\\ v_{n+} & 1\end{bmatrix}\\ mbix_+&=\begin{bmatrix}D\\ T_c+w\end{bmatrix} \end{aligned} \tag{10}$$

where $\boldsymbol{T}_{\mathrm{data}+}$ is a vector of torque reference inputs, $\boldsymbol{A}_+$ is a matrix of motor speeds, and $\boldsymbol{x}_+$ is a vector consisting of viscous friction, Coulomb friction and constant torque disturbance. Solving (10) for $\boldsymbol{x}_+$ using least square method yields

$$\boldsymbol{x}_+=(\boldsymbol{A}_+^{\mathrm{T}}\boldsymbol{A}_+)^{-1}\boldsymbol{A}_+^{\mathrm{T}}\boldsymbol{T}_{\mathrm{data}+}. \tag{11}$$

Next, let $T_{\mathrm{ref1}}-,T_{\mathrm{ref2}}-,\ldots,T_{\mathrm{refn}}-$ be torque reference inputs for negative motor speeds $v_{1-},v_{2-},\ldots,v_{n-}$, respectively. Following the similar procedure as in (8)–(11) yields

$$\begin{aligned} \boldsymbol{x}_-&=(\boldsymbol{A}_-^{\mathrm{T}}\boldsymbol{A}_-)^{-1}\boldsymbol{A}_-^{\mathrm{T}}\boldsymbol{T}_{\mathrm{data}-}\\ \boldsymbol{T}_{\mathrm{data}-}&=\begin{bmatrix}T_{\mathrm{ref1}}-\\ \vdots\\ T_{\mathrm{refn}-}\end{bmatrix},\boldsymbol{A}_-=\begin{bmatrix}v_1- & 1\\ \vdots & \vdots\\ v_{n-} & 1\end{bmatrix},\\ \boldsymbol{x}_-&=\begin{bmatrix}D\\ -T_c+w\end{bmatrix}. \end{aligned} \tag{12}$$

Coulomb friction T_c is obtained from (11) and (12) as

$$\begin{bmatrix}0\\ T_c\end{bmatrix}=\frac{1}{2}(\boldsymbol{x}_+-\boldsymbol{x}_-). \tag{13}$$

Likewise viscous friction D and constant torque disturbance w are obtained from (11) and (12) as

$$\begin{bmatrix}D\\ w\end{bmatrix}=\frac{1}{2}(\boldsymbol{x}_++\boldsymbol{x}_-). \tag{14}$$

E. Control and Reference Input

Control parameters used in simulations and experiments are given in Table III. The control parameters are based on the default values of the driver used in systems 1 and 2.

The parameters of position reference input are given in Table IV. Sinusoidal signals are used as position reference input in the following simulations and experiments. Both in simulations and experiments the frequency of position reference input ω is varied from $\omega_{\min}$ to $\omega_{\max}$ by $\Delta\omega$ increment, and for each ω moment of inertia is identified using (5). The upper bound of the frequency of position reference input $\omega_{\max}$ is selected such that position reference input has at least five sampling points per period when a controller operating at sampling time of 1 ms is used to generate position reference input as common in servo products. Since at the beginning of motion the effects of the transition from maximum static friction to dynamic friction appear in torque reference input and motor position, those signals between the eighth and the tenth period after the start of motion are used in the following simulations and experiments that is 1 s of torque reference input and motor position are taken for the identification when the frequency ω is 10 Hz. The amplitude of position reference input r_0 is selected such that the amplitude of motor position becomes less than 1/6 rotation to verify the applicability of the proposed algorithm to mechatronic servo systems with limited stroke.

F. Simulation and Experimental Results

Fig. 4 shows simulation results and experimental results of system 1. The solid lines represent experimental results and the dashed lines represent simulation results. Fig. 4(a) shows amplitude of motor position for varying frequency ω. Both in simulation and experiment the amplitude of motor position decreases as the frequency ω increases since the motor position cannot track the position reference input as its frequency increases.

TABLE IV
PARAMETERS OF POSITION REFERENCE INPUT

Lower bound of the frequency of position reference input ω_{min}	$10(2\pi)$ *rad / s*
Upper bound of the frequency of position reference input ω_{max}	$200(2\pi)$ *rad / s*
Increment of the frequency of position reference input $\Delta\omega$	$10(2\pi)$ *rad / s*
Amplitude of position reference input r_0	1 *rad*

Fig. 4(b) shows the amplitude of torque reference input for varying frequency ω. As frequency ω is increased, the amplitude of torque reference input in simulation and experiment increases and converges to 18.6% and 20.3% of rated torque, respectively. As in Fig. 4(a), the amplitude of motor position decreases as frequency ω increases and position tracking error increases. For larger position tracking error the controllers generate larger torque reference input to reduce the tracking error. At higher frequency ω the amplitude of motor position converges to zero, and the amplitude of position tracking error converges to the amplitude of position reference input. As a result, the amplitude of torque reference inputs in simulation and experiment increases and converges to constant values as in Fig. 4(b). The amplitude of torque reference input in experiment converges to a value 1.7% larger than the value in simulation because of unmodeled part of the system such as the gain of current loop.

Fig. 4(c) shows moment of inertia identification error for varying frequency ω. Moment of inertia identification error $e_J(\%)$ is calculated by (15) using identified moment of inertia J in (5) and true value of moment of inertia J^* in Table I

$$e_J = \frac{J - J^*}{J^*} \times 100. \tag{15}$$

In simulation the identification error is within $\pm 3\%$ for frequency ω between 10 Hz and 200 Hz whereas in experiment the identification error is within $\pm 12\%$. Although as mentioned in the earlier section, the frequency components such as subharmonics and superharmonics due to Coulomb friction can be eliminated by using the fundamental frequency component of torque reference input and motor position in identification calculation, Coulomb friction also has some contributions to the fundamental frequency component of torque reference input and motor position. Thus, in simulation the identification error is not exactly zero due to some contributions from Coulomb friction. For the same reason, in experiment Coulomb friction, and some additional noise in torque reference input and motor position caused some identification error.

The identification was repeated five times at $\omega = 100$ Hz where the amplitude of motor position in experiment is 0.025 rad that is 1/250 rotation, an example of a small stroke. Then the repeatability with respect to the average of five identification errors becomes $+1\%, -2\%, 0\%, +2\%$ and -1%.

Fig. 5 shows simulation results and experimental results of system 2. In Fig. 5(a) the amplitude of motor position decreases as frequency ω increases both in simulation and experiment for the same reason as in Fig. 4(a). The simulation result and experimental result have the same trend. Since backlash that exists in system 2 is not taken into account in the simulation model, time average of moment of inertia connected to the motor in experiment is slightly smaller than that in simulation. Consequently amplitude of motor position in experiment is slightly larger than the one in simulation. Since moment of inertia of system 2 is larger than that of system 1 as in Tables I and II, the amplitude of motor position in Fig. 5(a) is smaller than the one in Fig. 4(a).

Fig. 5(b) shows the amplitude of torque reference input. Both in simulation and experiment the amplitude of torque reference input decreases and approaches to a constant value as the frequency ω is increased. To explain the difference of the trend of the amplitude of torque reference input in Fig. 4(b) and Fig. 5(b), damping ratio and damped natural frequency of the closed loop system in Fig. 2 are analyzed. Approximating system 2 as an SDOF system the characteristics equation of the closed loop system in Fig. 2 is obtained from (1) and the expression of torque reference input in (16) as

$$T_{\text{ref}} = K_{\text{vj}}\left(1 + \frac{1}{T_i}\int dt\right)[K_p(r-\theta) - \dot{\theta}] \tag{16}$$

$$Js^3 + (D + K_{\text{vj}})s^2 + K_{\text{vj}}\left(K_p + \frac{1}{T_i}\right)s + \frac{K_p K_{\text{vj}}}{T_i} = 0 \tag{17}$$

where r is position reference input. If the system is underdamped, the characteristics equation (17) has one real root and a pair of complex conjugate roots expressed as $s = -\sigma \pm j\omega_d$ with $\sigma = \zeta\omega_n$, $\omega_d = \omega_n\sqrt{1-\zeta^2}$ where ω_n is undamped natural frequency and ζ is damping ratio. Real part σ represents rate of convergence and imaginary part ω_d represents damped natural frequency. Damping ratio is expressed using σ and ω_d as

$$\zeta = \frac{\sigma}{\sqrt{\omega_d^2 + \sigma^2}}. \tag{18}$$

For system 1 damped natural frequency and damping ratio are computed using the values in Table I as $\omega_d = 11.9(2\pi)$ rad/s and $\zeta = 0.83$, whereas those for system 2 are computed using the values in Table II as $\omega_d = 10.7(2\pi)$ rad/s and $\zeta = 0.19$. Damping ratio of system 2 is much smaller than that of system 1 because moment of inertia of system 2 is 4.79 times as large as that of system 1 as in Tables I and II. As damping ratio of system 2 is small, system 2 behaves in a vibrating manner near 10.7 Hz. To suppress the vibrations near 10.7 Hz the amplitude of torque reference input increases near $\omega = 10(2\pi)$ rad/s.

Fig. 5(c) shows moment of inertia identification error for varying frequency ω. In simulation the identification error is within $\pm 20\%$ for the frequency ω between 10 Hz and 200 Hz whereas in experiment the identification error is within $\pm 25\%$ for the frequency ω between 10 Hz and 200 Hz. Because of backlash that exists in system 2 the time average of the load moment of inertia connected to the motor is smaller than moment of inertia of the slider and the coupling. As a result the identified moment of inertia in experiment is smaller than that in simulation. Both in simulation and experiment the identified moment of inertia grow gradually as frequency ω increases. The gradual increase of the identified moment of inertia is due

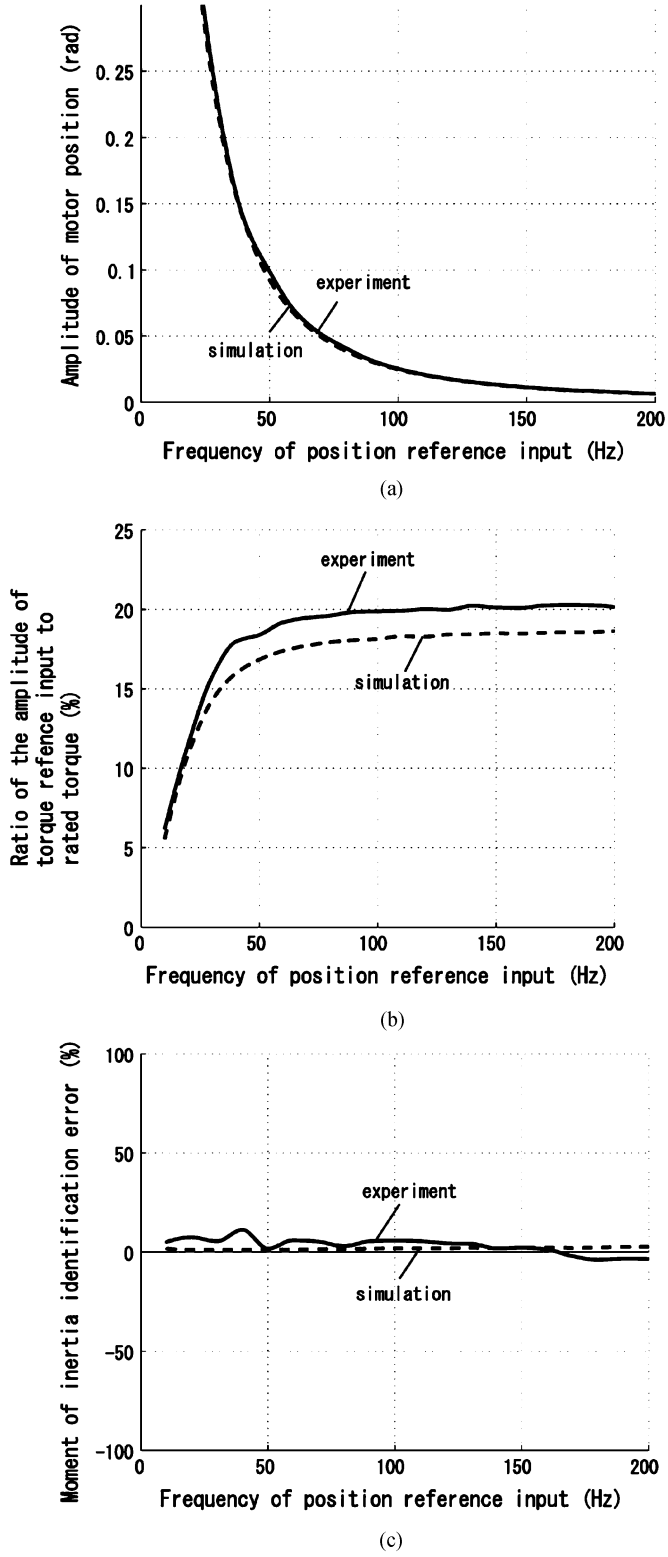

Fig. 4. Simulation results and experimental results of system 1. (a) Amplitude of motor position. (b) Amplitude of torque reference input. (c) Moment of inertia identification error.

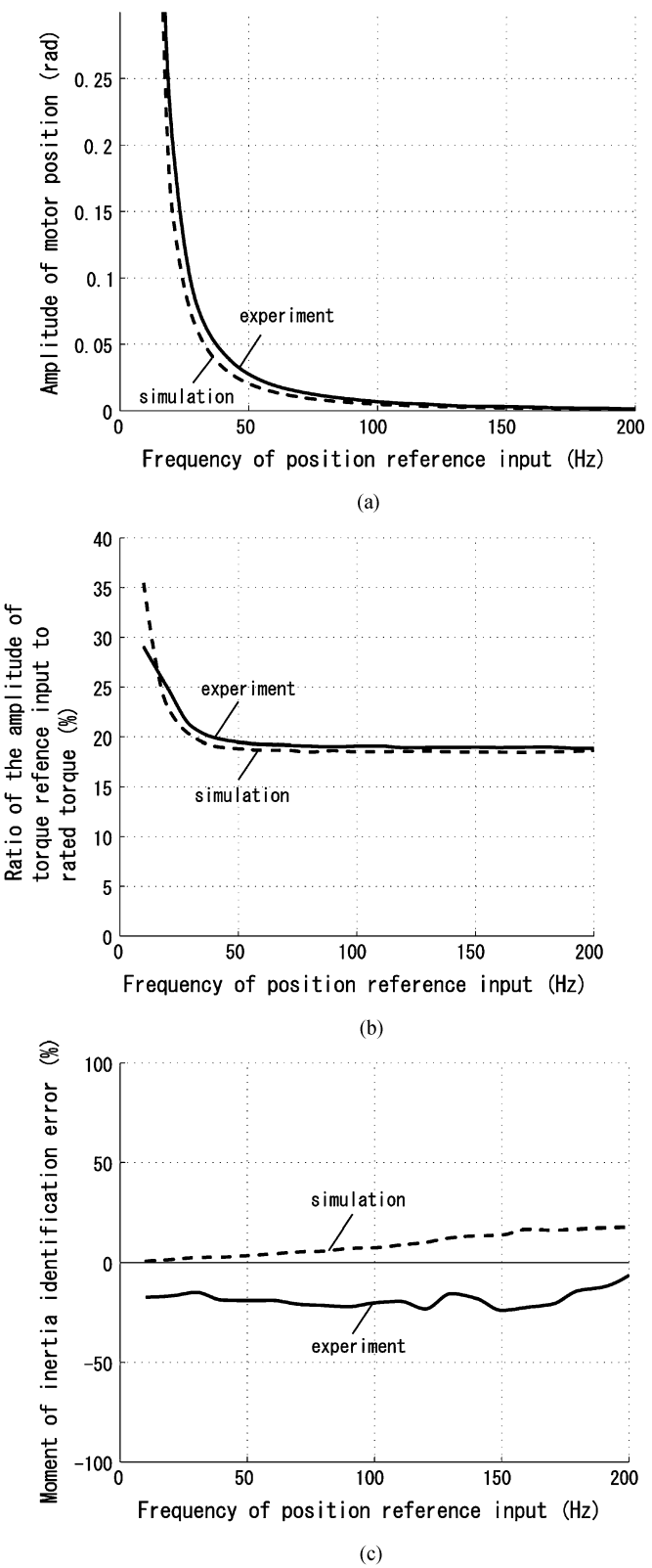

Fig. 5. Simulation results and experimental results of system 2. (a) Amplitude of motor position. (b) Amplitude of torque reference input. (c) Moment of inertia identification error.

to the fact that the contributions of elastic body dynamics is increasing and the amplitude of motor position is decreasing more rapidly than that of a pure SDOF system as frequency ω approaches antiresonance of system 2 at 402.3 Hz. Since identified moment of inertia in experiment is smaller than its true value due to backlash, it approaches the true value as frequency ω increases, and identification error decreases.

TABLE V
SUMMARY (SIMULATION RESULTS ARE IN PARENTHESIS)

System	Identification error (%)	Repeatability (%)	Identification time (s)	Frequency of position reference input suitable for identification (Hz)	Amplitude of motor position suitable for identification (rad)
1	±12 (±3)	±2	≤1 (≤1)	10 to 200 (10 to 200)	0.006 to 0.61 (0.006 to 0.62)
2	±25 (±20)	±3	≤1 (≤1)	10 to 200 (10 to 200)	0.001 to 0.83 (0.001 to 0.95)

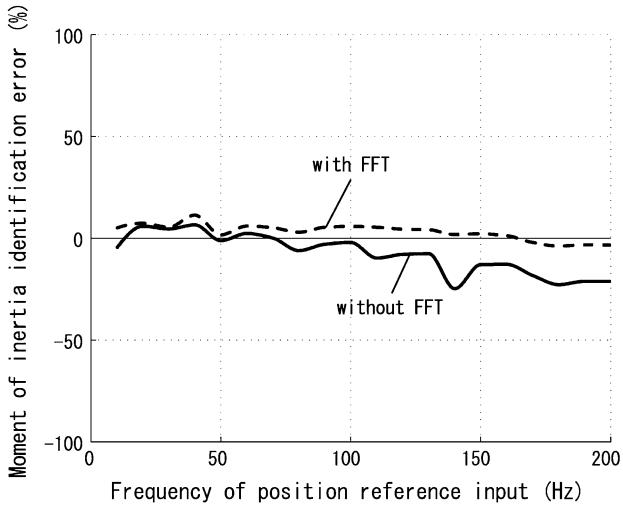

Fig. 6. Effect of FFT on identification results of system 1.

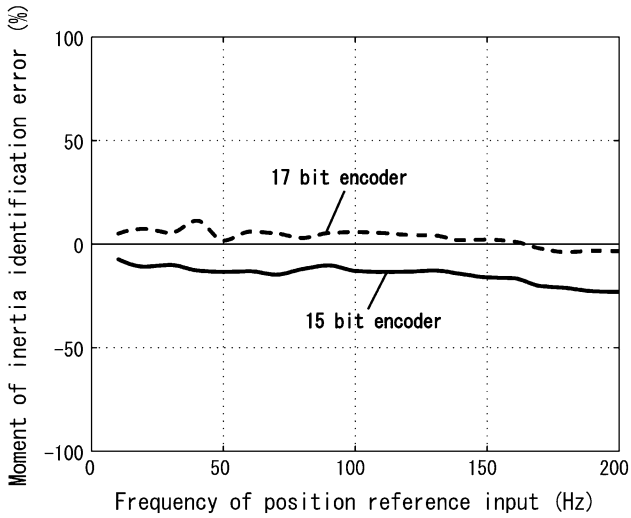

Fig. 7. Encoder resolutions and identification results of system 1.

Since the proposed identification algorithm assumes SDOF systems, the identification result has less influence from elastic body dynamics for the frequency ω sufficiently lower than antiresonance and resonance frequencies.

The identification was repeated five times at $\omega = 50$ Hz where the amplitude of motor position in experiment is approximately 0.025 rad that is 1/250 rotation, an example of a small stroke. Then the repeatability with respect to the average of five identification errors becomes $+3\%, -2\%, -3\%, +1\%$ and $+1\%$.

As mentioned in Section II, fundamental frequency component of torque reference input and that of motor position are extracted by FFT, and are used in identification (5). The proposed identification algorithm is used off line, especially during the preparatory period immediately after the mechatronic servo system is turned on and before the normal operation starts. Generally short preparatory period is preferred, however the shorter the preparatory period is the larger the transient response is. As mentioned in the advantage 4 in Section II, FFT is applied to torque reference input and motor position to eliminate the transient response of those signals. Fig. 6 shows the effect of FFT on the identification results of system 1. The solid line represents the identification error when FFT is not applied to the signals, and the dashed line represents the identification error when FFT is applied. The identification error without FFT is close to the one with FFT at low frequency, and the one without FFT decreases as frequency ω increases whereas the one with FFT remains almost constant. As mentioned earlier, torque reference input and motor position between the eighth and the tenth period after the start of motion are used in the identification. The time of ten periods is shorter as frequency ω increases whereas rate of decay of transient response remains constant. Therefore, at higher frequency ω torque reference input and motor position used in the identification contain more transient responses, and the identification error without FFT shows the growing influence of the transient response at higher frequency ω whereas the one with FFT eliminates the effect of transient response.

Fig. 7 shows the effect of encoder resolution on the identification results of system 1. The solid line represents the results with 15 b encoder, and the dashed line represents the results with 17 b encoder. Since today's standard servo products are equipped with 20 b encoder, and the lowest-specification products are with 15 b encoder, 15 b and 17 b encoders are employed in the experiment to illustrate that the proposed algorithm can be used with relatively low resolution encoders as mentioned in advantage 5. Motor position measured by 15 b encoder is four times as rough as the one measured by 17 b encoder, however even with 15 b encoder the identification error stays within $\pm 23\%$.

Results are summarized in Table V. With the proposed algorithm moment of inertia of system 1 is identified within $\pm 12\%$ error and $\pm 2\%$ repeatability whereas moment of inertia of system 2 is identified within $\pm 25\%$ error and $\pm 3\%$ repeatability. The proposed algorithm is derived for SDOF systems and gives the best results when elastic body dynamics is not dominating. The identification error of system 2 in experiment is due to elastic body dynamics and backlash nonlinearity that is not taken into account in the identification equation (5). The identification error of $\pm 25\%$ is common in the system

identification function of today's servo products, and is sufficient for use as a part of full automatic tuning of control gains for mechatronic servo systems with limited strokes. The time for calculating (5) is negligible compared with the time for taking torque reference input and motor position data. As mentioned earlier, torque reference input and motor position between the eighth and the tenth period after the start of motion are used in the identification. Therefore, the time for taking torque reference input and motor position data is less than or equal to 1 s when the frequency of position reference input is greater than or equal to 10 Hz. In practice, the frequency of position reference input is set to a value sufficiently lower than antiresonance of the system to be controlled but sufficiently high such that the amplitude of motor position is smaller than the allowable stroke. If the frequency of position reference input is set to 50 Hz as one of the examples of such value for system 2, the time for taking torque reference input and motor position data is 0.2 s.

Frequency of position reference input suitable for identification is the range of frequency ω with which the identification errors for systems 1 and 2 are within $\pm 12\%$ and $\pm 25\%$ in experiment and $\pm 3\%$ and $\pm 20\%$ in simulation, respectively. As mentioned earlier, the frequency used in practice is selected based on the amplitude of motor position and antiresonance frequency. If the allowable stroke is 1/250 rotation, 100 Hz and 50 Hz are the frequencies that can be used for systems 1 and 2, for instance.

Amplitude of motor position suitable for identification is the range of the amplitude of motor position with which the identification errors for systems 1 and 2 are within $\pm 12\%$ and $\pm 25\%$ in experiment and $\pm 3\%$ and $\pm 20\%$ in simulation, respectively. The results imply that with the proposed algorithm moment of inertia can be identified with less than 1/1000 rotation, and the proposed algorithm can be applied to mechatronic servo systems with limited strokes.

IV. Conclusion

In this paper, a moment of inertia identification algorithm for mechatronic servo systems with limited strokes is introduced. Simulations and experiments based on an electric motor and a linear slider are presented to demonstrate the applicability of the proposed algorithm to SDOF systems and 2 DOF systems. The main points are summarized as follows.

1) Moment of inertia is identified within $\pm 25\%$ error.
2) Identification is completed within 1 s.
3) The proposed algorithm can be used to identify moment of inertia of mechatronic servo systems with limited strokes.
4) Frequency of position reference input is selected such that amplitude of motor position is less than the allowable stroke and elastic body dynamics is not dominating.

References

[1] C. M. Liaw, R. Y. Shue, H. C. Chen, and S. C. Chen, "Development of a linear brushless dc motor drive with robust position control," *Proc. Inst. Elect. Eng.*, vol. 148, no. 2, pp. 111–118, Mar. 2001.

[2] M. W. Dunnigan, S. Wade, B. W. Williams, and X. Yu, "Position control of a vector controlled induction machine using Slotine's sliding mode control approach," *Proc. Inst. Elect. Eng.*, vol. 145, no. 3, pp. 231–238, May. 1998.

[3] F. Lin, "Fuzzy adaptive model-following position control for ultrasonic motor," *IEEE Trans. Power Electron.*, vol. 12, no. 2, pp. 261–268, Mar. 1997.

[4] W. C. Gan and N. C. Cheung, "Development and control of a low-cost linear variable-reluctance motor for precision manufacturing automation," *IEEE/ASME Trans. Mechatronics*, vol. 8, no. 3, pp. 326–333, Sep. 2003.

[5] X. Qian, Y. Wang, and M. L. Ni, "Robust position control of linear brushless DC motor drive system based on /spl mu/-synthesis," *Proc. Inst. Elect. Eng.*, vol. 152, no. 2, pp. 341–351, Mar. 2005.

[6] C. Attalaianese, A. Perfetto, and G. Tomasso, "Robust position control of dc drives by means of H infinity controllers," *Proc. Inst. Elect. Eng.*, vol. 146, no. 4, pp. 391–396, Jul. 1999.

[7] Y. Han, Y. Kim, J. Chol, and H. Woo, "The position control of induction motors using the binary disturbance observer," in *IECON '98. Proc. 24th Annu. Conf. IEEE Ind. Electron. Soc.*, Aachen, Germany, 31 Aug.–4 Sept. 1998, vol. 3, pp. 1457–1463.

[8] A. J. Helmicki, C. A. Jacobson, and C. N. Nett, "Least squares methods for h-infinity control-oriented system identification," *IEEE Trans. Autom. Control*, vol. 38, no. 5, pp. 819–826, May. 1993.

[9] A. J. Fleming and S. O. R. Moheimani, "Spatial system identification of a simply supported beam and a trapezoidal cantilever plate," *IEEE Trans. Control Syst. Technol.*, vol. 11, no. 5, pp. 726–736, Sep. 2003.

[10] W. Spinelli, L. Piroddi, and M. Lovera, "On the role of prefiltering in nonlinear system identification," *IEEE Trans. Autom. Control*, vol. 50, no. 10, pp. 1597–1602, Oct. 2005.

[11] V. Saligrama, "A convex analytic approach to system identification," *IEEE Trans. Autom. Control*, vol. 50, no. 10, pp. 1550–1566, Oct. 2005.

[12] L. Ljung, "Issues in system identification," *IEEE Control Syst. Mag.*, vol. 11, no. 1, pp. 25–29, Jan. 1991.

[13] K. Poolla and A. Tikku, "On the time complexity of worst-case system identification," *IEEE Trans. Autom. Control*, vol. 39, no. 5, pp. 944–950, May 1994.

[14] J. Chen, C. N. Nett, and M. K. H. Fan, "Worst case system identification in H infinity: Validation of *a priori* information, essentially optimal algorithms, and error bounds," *IEEE Trans. Autom. Control*, vol. 40, no. 7, pp. 1260–1265, Jul. 1995.

[15] A. S. McCormack, K. R. Godfrey, and J. O. Flower, "Design of multilevel multiharmonic signals for system identification," , *Germany*, vol. 142, no. 3, pp. 247–252, May. 1995.

[16] J. J. Barve and V. S. S. R. Junnuri, "System identification using transfer matrix," in *Proc. 2004 IEEE Conf. Robotics, Autom. Mechatronics*, Singapore, Dec. 1–3, 2004, vol. 2, pp. 1124–1129.

[17] G. P. Rao and H. Unbehauen, "Identification of continuous-time systems," *Proc. Inst. Elect. Eng.*, vol. 153, no. 2, pp. 185–220, Mar. 13, 2006.

[18] T. W. Flint and R. J. Vaccaro, "Performance analysis of N4SID state-space system identification," in *Proc. 1998 Amer. Control Conf. (ACC)*, Philadelphia, PA, Jun. 24–26, 1998, vol. 5, pp. 2766–2767.

[19] M. Kaneyoshi, H. Tanaka, M. Kamei, and H. Furuta, "New system identification technique using fuzzy regression analysis," in *Proc. 1st Int. Symp. Uncertainty Modeling Analysis, 1990*, Dec. 3–5, 1990, pp. 528–533.

[20] K. N. Lou and T. H. Fan, "A new multichannel spectral approach for system identification," in *Proc. IEEE Int. Conf. Syst. Engineering, 1992*, Sep. 17–19, 1992, pp. 311–314.

[21] T. W. S. Chow, G. Fei, and Y. F. Yam, "Application of modified sigma-pi-linked neural network to dynamical system identification," in *Proc. 3rd IEEE Conf. Control Applications, 1994*, Aug. 24–26, 1994, vol. 3, pp. 1729–1733.

[22] H. A. Barker, "Design of multilevel pseudorandom signals for specified harmonic content," in *Proc. IEE Colloquium Multifrequency Testing For Syst. Identification,* , London, U.K., Jun. 8, 1990, pp. 2/1–2/6.

[23] T. Long, Z. Sun, and C. Li, "Optimal experiment design for wavelet-based system identification," in *Proc. 4th World Congr. Intelligent Control Autom.*, Shanghai, China, Jun. 10–14, 2002, vol. 1, pp. 89–93.

[24] A. Forrai, S. Hashimoto, H. Funato, and K. Kamiyama, "Structural control technology: System identification and control of flexible structures," *Comput. Control Eng. J.*, vol. 12, no. 6, pp. 257–262, Dec. 2001.

[25] C. Hu, X. Huang, J. Hu, and J. Zhu, "System identification of a small uav's speeding up process before take-off," in *2004 5th Asian Control Conf.*, Melbourne, Australia, Jul. 20–23, 2004, vol. 1, pp. 392–395.

[26] N. Y. N. Chen and J. S. Gibson, "Subspace system identification using a multichannel lattice filter," in *Proc. 2004 Amer. Control Conf.*, Jun. 30–July 2 2004, vol. 1, pp. 855–860.

[27] H. A. Barker, A. H. Tan, and K. R. Godfrey, "Criteria for determining the optimal levels of multilevel perturbation signals for nonlinear system identification," in *Proc. 2003 Amer. Control Conf.*, Denver, CO, Jun. 4–6, 2003, vol. 5, pp. 4409–4414.

[28] B. Li, R. Wang, Y. Zhang, and Z. Wang, "Modeling of steering system of high speed intelligent vehicle by system identification," in *Proc. IEEE Int. Vehicle Electron. Conf. (IVEC'99)*, Changchun, China, Sep. 6–9, 1999, vol. 1, pp. 243–246.

[29] I. Awaya, Y. Kato, I. Miyake, and M. Ito, "New motion control with inertia identification function using disturbance observer," in *Proc. 1992 Int. Conf. Ind. Electronics, Control, Instrumentation, Autom.*, San Diego, CA, Nov. 9–13, 1992, vol. 1, pp. 77–81.

[30] N. Kim, H. Moon, D. Lee, and D. Hyun, "Inertia identification for the speed observer of the low speed control of induction machines," in *Conf. Rec. 1995 IEEE Ind. Applicat. Conf. 30th IAS Annu. Meeting*, Orlando, FL, Oct. 8–12, 1995, vol. 3, pp. 1938–1943.

[31] N. Kim, H. Moon, and D. Hyun, "Inertia identification for the speed observer of the low speed control of induction machines," *IEEE Trans. Ind. Appl.*, vol. 32, no. 6, pp. 1371–1379, Nov.–Dec. 1996.

[32] K. B. Lee, J. Y. Yoo, J. H. Song, and I. Choy, "Improvement of low speed operation of electric machine with an inertia identification using ROELO," *Proc. Inst. Elect. Eng.*, vol. 151, no. 1, pp. 116–120, Jan. 9, 2004.

[33] K. Ohishi and Y. Nakamura, "Robust self-tuning speed servo system for wide speed range based on instantaneous speed observer and disturbance observer," in *Conf. Rec. 1996 IEEE Ind. Applicat. Conf. 31st IAS Annu. Meeting*, San Diego, CA, Oct. 6–10, 1996, vol. 1, pp. 339–346.

[34] K. Lee, J. Song, I. Choy, and J. Yoo, "An inertia identification using ROELO for low speed control of electric machine," in *Proc. 18th Annu. Appl. Power Electron. Conf.*, Miami Beach, FL, Feb. 9–13, 2003, vol. 2, pp. 1052–1055.

[35] S. Yang and Y. Deng, "Observer-based inertial identification for auto-tuning servo motor drives," in *Conf. Rec. 2005 IEEE Ind. Applicat. Conf. 40th IAS Annu. Meeting*, Hong Kong, China, Oct. 2–6, 2005, vol. 2, pp. 968–972.

[36] K. Ohishi and Y. Nakamura, "Robust speed servo system for wide speed range based on instantaneous speed observer and disturbance observer," in *Proc. 4th IEEE Int. Workshop Adv. Motion Control - AMC '96 - MIE*, Mie, Japan, Mar. 18–21, 1996, vol. 1, pp. 326–331.

[37] S. Hong, H. Kim, and S. Sul, "A novel inertia identification method for speed control of electric machine," in *Proc. 1996 IEEE IECON. 22nd Int. Conf. Ind. Electronics, Control, Instrum.*, Taipei, Taiwan, R.O.C., Aug. 5–10, 1996, vol. 2, pp. 1234–1239.

[38] Y. Guo, L. Huang, and M. Muramatsu, "Research on inertia identification and auto-tuning of speed controller for AC servo system," in *Proc. Power Conversion Conf. - Osaka PCC 2002*, Osaka, Japan, Apr. 2–5, 2002, vol. 2, pp. 896–901.

[39] Y. Guo, L. Huang, Y. Qiu, and M. Muramatsu, "Inertia identification and auto-tuning of induction motor using MRAS," in *Proc. 3rd Int. Conf. Power Electron. Motion Control*, Beijing, China, Aug. 15–18, 2000, vol. 2, pp. 1006–1011.

[40] A. K. Sanyal, M. Chellappa, J. L. Valk, J. Ahmed, J. Shen, and D. S. Bernstein, "Globally convergent adaptive tracking of spacecraft angular velocity with inertia identification and adaptive linearization," in *Proc. 42nd IEEE Int. Conf. Decision Control*, Maui, HI, Dec. 9–12, 2003, vol. 3, pp. 2704–2709.

[41] D. Karnopp and R. C. Rosenberg, *Analysis and Simulation of Multiport Systems: The Bond Graph*. New York: MIT Press, 1968.

Fukashi Andoh (M'06) received the Ph.D. degree in mechanical engineering from Ohio State University, Columbus, in 2001.

In 2002 and 2003, he was a Visiting Scholar with the Department of Mechanical Engineering, Ohio State University. Since 2004, he has been with YASKAWA Electric Corporation. His current research interests are system identification, control of mechatronic servo systems, vibration control, control of distributed parameter systems, and control of delayed systems.